# THE ROLE OF CARBIDES IN THE CORROSION BEHAVIOR OF FE-12CR-1MOVW STEEL IN LIQUID LITHIUM

G. E. Bell and M. A. Abdou
Department of Mechanical, Aerospace and Nuclear Engineering
University of California at Los Angeles
Los Angeles, CA 90024-1597
(213) 206-1228

## ABSTRACT

Experimental investigations with lithium and Fe-12Cr-1MoVW alloy in two thermal convection loops (360 to 505°C and 530 to 655°C) have shown that weight changes in these systems are not simple increasing functions of temperature. It was found that redistribution of carbon from the α-ferrite phase of the isothermally annealed material by the formation of large (10-20 μm in diameter) surface carbides with the crystallographic structure of $M_{23}C_6$ (M=Fe or Cr) dominate the weight changes between 450 and 580°C. The release of carbon from the surface α-ferrite is probably due to decreased surface chromium activity by the formation of $Li_9CrN_5$ in the lower temperature experiment. In the higher temperature experiment, the difference in carbon activity between the steel and lithium is probably due to the rapidly increasing solubility of carbon in the lithium. The stoichiometry of the surface carbides varied from $Cr_{18.8}Fe_{4.2}C_6$ to $Cr_{3.2}Fe_{19.8}C_6$ with temperature and loop position, while surface substrate chromium content ranged from 4 to 8% by weight, decreasing with increasing temperature. Controlling initial chromium and carbon activities in the steel by decreasing carbon contents and/or by substituting more stable carbide-forming elements such as titanium or vanadium for chromium could help to mitigate the problem.

## I. INTRODUCTION

Because of its excellent heat transfer and tritium breeding characteristics, lithium is an attractive coolant and breeder material for D-T fusion reactors. However, austenitic steels exposed to lithium can suffer severe corrosion due to high solubility of certain alloy constituents[1] in lithium and/or the interaction of the alloy components with dissolved nonmetallic elements in the lithium [2]. Data from ferritic steel alloys, such as Fe-12Cr-1MoVW[3], showed that the magnitude of corrosion by lithium , in terms of weight loss at a given temperature, was not as severe as for austenitic steels. Resulting weight change profiles from thermal convection loop experiments[4,5,6] differed substantially from the profiles found in lithium/austenitic steel systems. This paper presents data and analysis of the surface morphology, chemistry and crystallography data which resulted from two thermal convection loop experiments with lithium and Fe-12Cr-1MoVW steel. Weight change, apparent corrosion rate and deposition rate data, as a function of temperature, are reported elsewhere[7].

## II. EXPERIMENTAL APPARATUS

A schematic of the thermal convection loops used in these investigations is shown in figure 1. The experiments are described in detail elsewhere[7]. Briefly, isothermally annealed, tubular specimens (approximately 38 mm long, 19 mm OD with 1.6 mm wall thickness) of an Fe-11.9Cr-1.0Mo-0.7Mn-0.4W-0.2V-0.1Si-0.4Ni-0.2C (wt%) alloy were exposed to lithium in two thermal convection loops (TCL's). The lithium was purified by filtering, cold trapping and hot gettering prior to filling the loops. The starting concentrations of oxygen and nitrogen in lithium were less than 200 and 30 wppm, respectively. One loop, designated GEB-1, operated for 3040 hour between 360 (633 K) and 505°C (778 K) and the other, designated GEB-2, for 2510 hours between 530 (803 K) and 655°C (928 K). After exposure, the specimens were examined using scanning electron microscopy (SEM and associated energy dispersive X-ray (EDX)), X-ray diffraction and electron microprobe analysis.

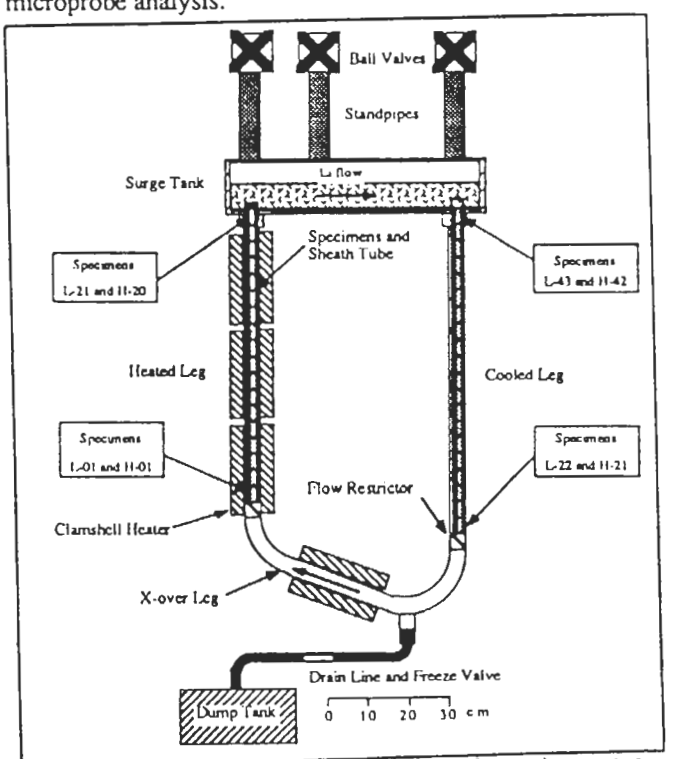


Fig. 1 Schematic of Thermal Convection Loop Apparatus

## III. EXPERIMENTAL RESULTS

### A. Surface Morphologies

Samples of the surface morphologies resulting from the specimen exposure to lithium are shown in figure 2. Specimens with temperatures below 450°C (723 K) in both the heated and cooled legs of GEB-1 were characterized by a roughened surface (Fig. 2 a). For specimens exposed to lithium with temperatures between 450 (723 K) and 505°C (778 K) in both the heated and cooled legs of GEB-1 and between 530 (803 K) and 580°C (853 K) in the cooled leg only of GEB-2, chromium-rich faceted nodules nucleated and grew on the surfaces exposed to lithium. The size and number density (number of nodules per unit area) of the chromium-rich nodules increased with increasing temperature in GEB-1. In GEB-2, the size and number density of the chromium-rich nodules increased with decreasing temperature to a maximum of approximately 20 μm. The chromium-rich nodules appeared first at the grain boundaries and eventually covered most of the surface (Fig. 2 b). The base metal under the chromium-rich nodules had the appearance of pebbles or cobblestones. The size of the cobblestones increased with temperature. In the heated leg of GEB-2, smaller, iron-rich nodules were found only on the first three specimens at the entrance of the flow to the heated leg (Fig. 2 c). The iron-rich nodules were smaller in size, had no apparent preferred orientation to the surface and were less faceted in appearance as compared to the chromium-rich nodules. The number density of the iron-rich nodules decreased rapidly with increasing temperature. No other specimens beyond the first three specimens in the heated leg of GEB-2 had any nodules, iron or chromium-rich, adhering to the surface. As the temperature further increased beyond 580°C (853 K) in GEB-2, the nodules disappeared from the surface completely. The cobblestone surface persisted as temperature increased with fluorescent, white speckles decorating some of the surfaces above 580°C (853 K) and up to the maximum temperature of 655°C (928 K) in GEB-2 (Fig. 2 d).

### B. X-ray Diffraction Analysis

X-ray diffraction analysis was performed on selected chromium and iron-rich nodule-bearing specimens. The resulting diffraction pattern was a combination of the diffraction lines of $Cr_{23}C_6$ (nodules) (lattice parameter $a=10.67 \pm 0.01$ Å) and a body-centered-cubic Fe/Cr alloy (base metal) (lattice parameter $a=2.878 \pm 0.003$ Å). Minor deviations of the diffraction pattern from that reported in the literature were found, but were probably due to the partial replacement of chromium with iron in the crystal structure. However, iron and chromium-rich nodule-bearing surfaces produced similar diffraction patterns indicating that both iron and chromium-rich nodules are metal carbides of the form $M_{23}C_6$ (M= Fe or Cr), although they differ in metallic composition, morphology and surface topography.

### C. Surface Composition

Figure 3 summarizes the EDX analysis results for surface composition which were collected from specimens examined with the SEM and associated semi-quantitative X-ray system. Data for the base metal (Fig. 3 a) are reported in terms of the chromium to iron ratio (Cr/Fe). Data for the carbide nodules are reported in terms of chromium atom stoichiometry, X, (Fig. 3 b) where X refers to equation {1}.

$$X\,Cr + (23\text{-}X)\,Fe + 6\,C \Leftrightarrow Cr_X\,Fe_{(23-X)}C_6 \quad \{1\}$$

Table 1 gives samples of the semi-quantitative compositions of from the EDX analysis for the specimens shown in Fig. 2. The base material showed depletion from the starting Cr/Fe ratio of 0.13 with the exception of the surfaces heavily populated with nodules (e.g. Fig. 2 b) in the cooled leg of GEB-2 which showed slight Cr/Fe enrichment in the original base metal composition. The nodules which formed were higher in chromium content than the original matrix with the

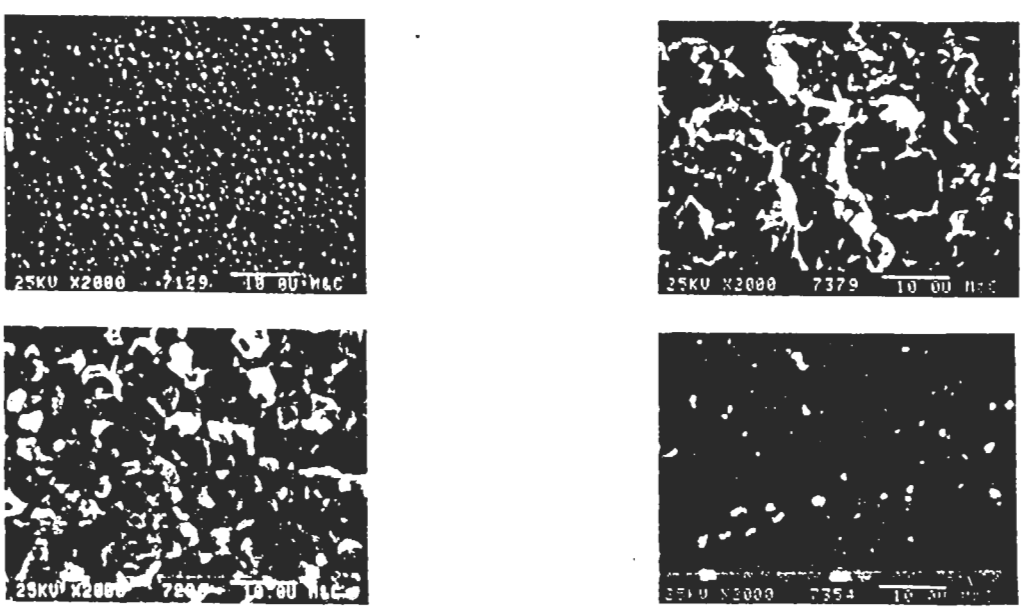


Fig. 2 Surface Morphologies: a) Roughened Surface (upper left) b) Chromium-rich Nodules (H-21) upper right) c) Fe-rich Nodules (lower left) d) Cobblestone Surface with fluorescent speckles (lower right)

exception of those at the entrance to the heated leg of GEB-2. The nodules in the cooled leg of GEB-2 were higher in chromium content than those in either the heated or cooled legs of GEB-1. The nodules in both GEB-1 and GEB-2 showed an increasing chromium stoichiometry, X, with increasing temperature up to a maximum followed by a decrease in X at the maximum temperature in GEB-1 and before the nodules disappeared in GEB-2. In addition, EDX analysis of the fluorescent, white speckles from specimens above 580°C showed them to be enriched in molybdenum and vanadium as compared to the base material. However, because of their small size, it was not possible to obtain accurate analysis of their composition.

D. Electron Microprobe Analysis

Electron microprobe depth profiles for chromium and iron of two selected specimens are shown in figure 4. Microprobe traces for specimen cross sections below 520°C showed no discernable affect on chromium or iron profiles due to exposure to lithium (not shown). The microprobe data show little effect on the substrate composition by the growth of surface nodules on the specimen (Fig. 4 a). Some increase in chromium concentration in the near surface region was detected, but the effected region is less that 2 μm deep and the resolution of the microprobe trace near the interface is questionable. Note that the microprobe traces were taken in the matrix and do not include surface nodules. At the higher temperatures, chromium depletion of the bulk material was evident, as shown in the microprobe trace for specimen H-19 (Fig. 4 b). The depth of the affected zone is approximately 8 to 10 μm with a sharp increase in chromium content at 10 μm. Cross sectional optical micrographs[7] showed the region of chromium depletion to correspond to the region of decarburization.

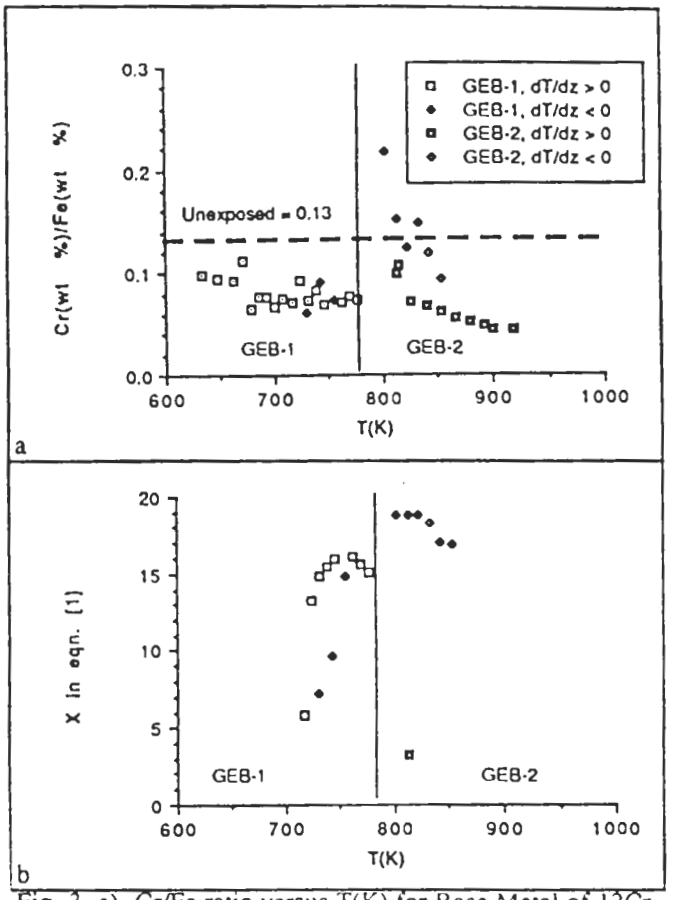


Fig. 3 a) Cr/Fe ratio versus T(K) for Base Metal of 12Cr-1MoVW Specimens Exposed to Lithium in TCL's b) X in equation (1) versus T(K) for Nodules Observed on 12Cr-1MoVW Specimens Exposed to Lithium in TCL's

| Specimen Identification | Temperature (°C) | Length of Exposure (hours) | EDX Composition (wt %) * Fe | Cr | Mo | Si | Ni |
|---|---|---|---|---|---|---|---|
| Unexposed | --- | --- | 85.9 | 11.5 | 1.1 | 0.4 | 0.4 |
| L-25 | 375 | 3040 | | | | | |
| Base Metal | | | 89.9 | 9.0 | 0.4 | 0.4 | 0.4 |
| H-21 | 530 | 2510 | | | | | |
| Base Metal | | | 81.5 | 17.7 | 0.2 | 0.4 | 0.3 |
| Chromium-rich Nodules** $\{Cr_{18.4}\ Fe_{4.6}C_6\}$ | | | 19.0 | 78.7 | 0.0 | 0.7 | 1.6 |
| H-01 | 540 | 2510 | | | | | |
| Base Metal | | | 90.2 | 8.8 | 0.2 | 0.6 | 0.3 |
| Iron-rich Nodules** $\{Cr_{3.2}\ Fe_{19.8}C_6\}$ | | | 85.1 | 12.9 | 0.6 | 0.4 | 0.4 |
| H-19 | 645 | 2510 | | | | | |
| Base Metal | | | 94.3 | 4.2 | 0.1 | 0.6 | 0.2 |

*The values shown represent the average of at least five analyses using semi-quantitative analysis. It was assumed that Fe, Cr, Mo, Ni and Si summed to 100%.

**The X-ray system is such that elements with mass numbers less than 20 cannot be detected. In particular, oxygen, nitrogen, carbon and lithium cannot be detected. These data are provided for comparison only.

Table 1: Base Metal and Nodule Composition for Specimens in Figure 2

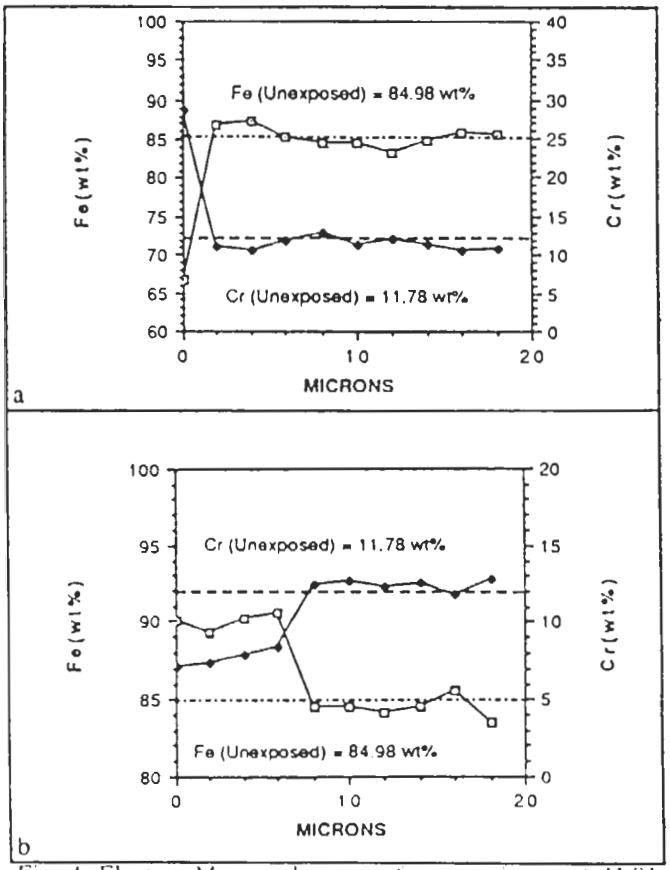


Fig. 4 Electron Microprobe traces from specimens a) H-01 (810 K) b) H-19 (920 K)

## IV. DISCUSSION AND ANALYSIS OF RESULTS

Most analyses of mass transfer in lithium/steel systems attempt to explain the observed surface morphology and weight change profiles in terms of solubilities of major alloy components. Since the solubilities of the steel constituents (e.g. iron, chromium, nickel, etc.) are non-zero and increase with temperature, mass transfer should be from the hotter to the cooler regions. If mass transfer were dominated by solubility, specimen weight losses should increase with increasing temperature. Indeed, surface morphology and weight change profiles of austenitic stainless steels in lithium are dominated by the preferential dissolution of nickel and reaction of chromium with dissolved nitrogen in the lithium. However, for Fe-12Cr-1MoVW, it appears from the results presented above that the behavior of metal carbides, both on the surface and in the bulk of the steel, influence the observed mass transfer processes and surface morphologies more than the solubilities of the major alloy components in lithium.

The behavior of Fe-12Cr-1MoVW in lithium is similar in some ways to the behavior of austenitic steels in lithium. Barker and Frankham[8] found evidence of $M_{23}C_6$ carbides along with the corrosion product $Li_9CrN_5$ on the ferrite layer formed by exposing type 316 stainless steel to lithium at 600°C with a constant carbon activity greater than 0.02 and nitrogen activities greater than $10^{-3}$. However, the carbide phase which formed was not as massive and was interspersed with the ferrite surface layer which formed due to the selective removal of nickel. Below 450°C, nitrogen activities in the lithium and chromium activities in the steel in these experiments were theoretically sufficient to permit formation of $Li_9CrN_5$[7]. However, no attempt to identify the corrosion product was made due to the difficulty of isolating the compound outside the lithium environment.

Tortorelli and DeVan[9] observed fluorescent molybdenum enriched "speckles" on the ferrite surface layer of type 316 stainless steel exposed to lithium in thermal convection loops at temperatures near 600°C that were similar to the speckles which formed on the grooved surface above 580°C in these experiments. The speckles observed here and by Tortorelli and DeVan are probably molybdenum/vanadium-containing precipitates that are exposed as the surface of the alloy recedes. Molybdenum and vanadium are less soluble in lithium as compared to iron and chromium and are therefore more resistant to dissolution.

Tortorelli[6] reported finding nodules of varying compositions on Fe-12Cr-1MoVW exposed to lithium which were similar to the nodules described here. Chopra[10,11] also reported nodules on pure chromium specimens exposed to lithium similar to the nodules described above. Both Tortorelli and Chopra originally interpreted the nodules as the remnants of the $Li_9CrN_5$ corrosion product which formed during exposure and subsequently decomposed during the specimen cleaning leaving behind chromium. Tortorelli indicated that pre-existing carbides at grain boundaries may have served as precursors for the formation of the nodules. However, Tortorelli concluded that the nodules themselves were not carbides because the nodules did not etch when viewed in cross section. Re-examinations of the chromium specimens by Chopra[12] with X-ray diffraction showed the deposits on the chromium specimens to be $M_{23}C_6$.

The faceted nature of the chromium-rich surface $M_{23}C_6$ carbide nodules and their initial, preferential nucleation along grain boundaries indicate that the carbides are being precipitated from the adjacent liquid phase. On the other hand, the iron-rich nodules did not exhibit any preferred orientation relative to the grains and/or grain boundaries and were less clearly faceted. It is possible that the flow disruption (i.e. flow restrictor) at the inlet to the heated leg of GEB-2 could have disrupted the boundary layer and increased the deposition rate of particles suspended in the flow causing this random surface distribution of iron-rich carbides on the surfaces. Chopra and Hull [13] also reported finding iron-rich carbides on the surfaces of ferritic steels exposed to lithium only at the downstream positions in their forced convection loop. Chemical analysis of unfiltered samples of lithium from both GEB-1 and GEB-2 showed iron and chromium levels in excess of the elemental solubilities. Chopra[12] also observed iron and chromium concentrations in excess of solubility levels in unfiltered samples of lithium from his forced convection loop experiments. However, Chopra's filtered samples showed a decrease in iron, chromium and carbon analyses. These results indicate that these metallic elements (Fe and Cr) may be in the form of particles as compounds, possibly, with carbon. However, if suspended particle deposition were the mechanism for iron-rich carbide deposition, then we would expect to find some iron-rich carbide nodules on all surfaces. This was not the case and iron-rich nodules appeared only at the inlet of the flow to the heated leg in GEB-2 which would correspond to Chopra and Hull's downstream position.

Carbon in the Fe-12Cr-1MoVW steel resides both in solid solution in the α-ferrite matrix and as dispersed, segregated metal carbides in the matrix or at grain boundaries. The heat treatment of the steel will determine the composition, distribution and type of carbide which forms. The solubility and activity of carbon in steel are strongly dependent on the composition of the steel (chromium content) and temperature. The activity of carbon in ferritic steels increases as the temperature increases and as the chromium content of the of the alloy decreases. Data available at 700°C from Fe-9Cr-Mo ferritic alloys show that saturation carbon concentrations in the ferrite matrix are less than 100 wppm[14]. Carbon was present in the initial alloy at approximately 0.2 wt% (2000 wppm) which means that most of the carbon in Fe-12Cr-1MoVW is in carbides dispersed in the matrix and precipitated at grain boundaries. At equilibrium, the activities of carbon in the α-ferrite matrix, $M_{23}C_6$-carbide and lithium are all equal. If activities are unequal, then transport of carbon will take place in the direction of decreasing carbon activity. Data specifically for carbon activity in Fe-12Cr-1MoVW alloys are not available but there are some data for austenitic steels[15]. Using the expression of Saltelli et al.[14] for chromium activity coefficient in the α-ferrite phase, we estimated the initial chromium activity of the α-ferrite below approximately 450 °C to have been nearly unity. Nitrogen levels in the lithium below 450°C (in GEB-1) were sufficient to allow the formation of $Li_9CrN_5$, which forms as a separate phase[2]. If we assume $Li_9CrN_5$ forms, then formation of $Li_9CrN_5$ on the α-ferrite phase of the surface decreases the surface chromium activity of the steel. The decrease in chromium activity increases the surface carbon activity of the α-ferrite phase. Carbon is, thus, released from the surface into the lower carbon activity lithium. Foramtion of $Li_9CrN_5$ may also decomposed chromium-rich $M_{23}C_6$ carbides on the surface of th steel which also releases carbon in to the lithium[7]. Since the solubility of carbon in lithium is low, small additions of carbon cause large changes in carbon activity. The carbon released from the surface of the steel is redistributed, via the flowing lithium, and the nodules form when the kinetics of the reaction are sufficient to allow. formation and/or the $Li_9CrN_5$ corrosion product cannot form. The bulk of the alloy is relatively unaffected because solid state diffusion is slow at the lower temperatures. The bulk of the alloy undergoes decarburization at the higher temperatures (Fig. 4 b). The phase boundary reaction between the carbides and thc steel matrix may also be limiting[14] even at higher temperatures. The nodules composition varies as the activities of the carbide components (most notably chromium [7]) varies around the loop. For a fixed carbon content in lithium, the activity of carbon in the liquid phase decreases as the temperature and saturation concentration increase[16]. Carbides will continue to precipitate so long as the carbon activity in the lithium is higher than in the activity of carbon in the precipitating $M_{23}C_6$ phase. If the carbon activity of the lithium drops sufficiently, carbides of any stoichiometry cannot form. Pillai and Mathews[15] found that the free energy of the mixed $M_{23}C_6$ for a given temperature was U-shaped with a minimum in free energy of formation between $18<X<19$. Such a minimum in free energy of formation is consistent with the shape of Fig. 3 b. The stoichiometry of the carbides found range from X= 3.2 to X=19.8.

The occurrence of these nodules over the fusion-relevant temperature range between 450 and 580°C is particularly important since such preferential deposition of material could cause flow restrictions and/or increased radiological hazards in fusion reactor designs utilizing ferritic steels and lithium. The formation of the carbide nodules represents a redistribution of carbon from the surface of the steel to carbides at grain boundaries because of the tendency of chromium to form a corrosion product with dissolved nitrogen in lithium. Darken and Ryba[17] showed that for ferritic steels, chromium significantly decreased steel carbon activity up to about 5 wt%. Vanadium and niobium are stronger carbide formers than chromium[18]. The use of significant amounts of niobium is undesirable from an activation standpoint[19]. Substitution of vanadium for some portion of the chromium in excess of the 5 wt% could substantially reduce the carbon activity and reduce the problem of surface carbon redistribution due to chromium removal while maintaining material strength.

## V. SUMMARY AND CONCLUSIONS

Experimental data have been collected from two thermal convection loop experiments with lithium and Fe-12Cr-1MoVW between 360 and 655°C. Results from the analysis of the specimens and these data from these experiments indicate that the corrosion processes are not controlled by the simple dissolution of the metal constituents from the solid to the liquid phase but are more dependent on the behavior of carbon and its compounds with metallic elements in liquid and solid phases.

From the results presented,we conclude the following:

1) At low temperatures, below 450°C, surface decarburization is probably induce by the decrease in chromium activity via the formation of $Li_9CrN_5$. Bulk diffusion is slow and decarburization is limited to the surface region.

2) The carbon released from the surface is redistributed to the nodules which begins at the grain boundaries where nucleation is preferred due to pre-existing carbides. Some of the released carbon may be in the form of carbide particles carried along by the flow.

3) At higher temperatures, carbon activities increase in the steel, decrease in liquid phase, solid phase diffusion increases and decarburization of the bulk steel is favored and surface carbide nodules are thermodynamically unstable towards the lower carbon activity in the lithium. The α-Fe/carbide phase boundary reaction may limit the bulk decarburization of the steel at temperatures below 650°C, although data are inconclusive in this respect.

4) Only by lowering the carbon activity by reducing the initial carbon content of the alloy and/or the substitution of stronger carbide forming alloy elements for chromium in the solid phase can the effect of carbide precipitation be limited.

## ACKNOWLEDGMENTS

The encouragement and suggestions of P. F. Tortorelli of Oak Ridge National Laboratory are gratefully acknowledged. This work was performed, in part, under U. S. Department of Energy grant number DE-FG03-86ER52123 and is based, in part, on worked performed in the laboratory graduate participation program under contract DE-AC05-76OR00033 between the U. S. Department of Energy and Oak Ridge Associated Universities.

[1]P. F. TORTORELLI AND J. H. DEVAN, "Mass Transfer Kinetics in Lithium-Stainless Steel Systems," Liquid Metal Engineering and Technology, BNES, London, (1985).

[2]M. G. BARKER, P. HUBBERSTEY, A. T. DADD AND S. A. FRANKHAM, "The interaction of Chromium with Dissolved Nitrogen in Liquid Lithium," J. Nucl. Mater., 114 (1983) 143-149.

[3]G. A. WHITLOW, W. L. WILSON, W. E. RAY AND M. G. DOWN, "Materials Behavior in Lithium Systems for Fusion Reactor Applications," J. Nucl. Mater., 85 & 86 (1979) 282-287.

[4]G. E. BELL, M. A. ABDOU AND P. F. TORTORELLI, "Experimental and Analytical Investigations of Mass Transport Processes of 12Cr-1MoVW Steel in Thermally-Convected Lithium Systems," presented at the International Symposium on Fusion Nuclear Technology, Tokyo, Japan, April 11-15, 1988.

[5]P. F. TORTORELLI AND J. H. DEVAN, "Corrosion of an Fe-12Cr1MoVW Steel in Thermally-convective Lithium," Proc. Topical Conf. Ferritic Alloys for use in Nuclear Energy Technologies, Snowbird, Utah, June 19-23, 1983, (1983) 215-221.

[6]P. F. TORTORELLI, "Corrosion of Ferritic Steels by Molten Lithium: Influence of Competing Thermal Gradient Mass Transfer and Surface Product Reactions," J. Nucl. Mater., 154-156 (1988).

[7]G. E. BELL, Thermal Convection Loop Experiments and Analysis of Mass Transport Processes in Lithium/Fe-12Cr-1MoVW Systems, Ph.D. Dissertation, University of California, Los Angeles, (1988).

[8]M. G. BARKER AND S. A. FRANKHAM, "The Effects of Carbon and Nitrogen on the Corrosion resistance of Type 316 Stainless Steel to Liquid Lithium," J. Nucl. Mater. 107 (1982) 218-221.

[9]P. F. TORTORELLI AND J. H. DEVAN, "Effects of a Flowing Lithium Environment on the Surface Morphology and Composition of Austenitic Stainless Steel," Microstructural Science, 12 (1982) 213-226.

[10]O. K. CHOPRA AND D. L SMITH, "Influence of Temperature and Lithium Purity on Corrosion of Ferrous Alloys in a Flowing Lithium Environment," Journal of Nuclear Materials, 141-143 (1986) 584-591.

[11]O. K. CHOPRA AND D. L SMITH, "Compatibility of Ferritic Steels in Forced Circulation Lithium and Pb-17Li Systems," Journal of Nuclear Materials, 155-157 (1988) 715-721.

[12]O. K. CHOPRA, Private Communication, April 1988.

[13]O. K. CHOPRA AND A. B. HULL, "Influence of Carbon and Nitrogen on Corrosion of Structural Materials in Flowing Lithium," ANS 8th Topical Meeting on the Technology of Fusion Energy, October 9-13, 1988, Salt Lake City, UT.

[14]A. SALTELLI, O. K. CHOPRA AND K. NATESAN, "An Assessment of the Carburization-Decarburization Behavior of Fe-9Cr-Mo Steels in a Sodium Environment," J. Nucl. Mater., 110 (1982) 1-10.

[15]S. R. PILLAI AND C. K. MATHEWS, "Carbon Potential and Carbide Equilibrium in 18/8 Austenitic Steel," J. Nucl. Mater., 150 (1987) 31-41.

[16]R. M. YONCO AND H. I. HOMA, "The Solubility of Carbon in Low-nitrogen Liquid Lithium," J.Nucl. Mater., 138 (1986) 117-22.

[17]L. S. DARKEN AND E. R. RYBA, "Metastable Phenomena in Hydrogen Degradation of Low Carbon Alloy Steels," EPRI AF-1176, Pennsylvania State University, September 1979.

[18]M. SMALL, "Theoretical Analysis of Carbon Cluster Formation in Solid Iron Based Alloys: A Review of the Alex-McLellan Mathematical Model," EPRI AP-1478, Pennsylvania State University, August 1980.

[19]P. F. TORTORELLI, Private Communication, September 1988.